Available online at www.sciencedirect.com

ScienceDirect

Procedia Engineering 10 (2011) 2937–2942

Engineering Procedia

ICM11

Effect of the experimental technique onto R dependence of ΔK_{th}

M. Carboni[a], D. Regazzi[a*]

[a] *Dept. Mechanical Engineering, Politecnico di Milano, Via La Masa 34, 20156 Milano, Italy*

Abstract

An experimental study on two structural steels (normalized C45 and 25CrMo4 grades) was conducted to determine the influence of the adopted technique onto the threshold SIF value. For both the tested materials, the standard approach used to pre-crack the specimens showed to have an influence on determining the thresholds, generating SIF higher than the ones estimated adopting compression pre-cracking techniques. This observation can have a huge effect on both life prediction and inspection intervals for a real structure. An example of life prediction was carried out applying the Nasgro equations, with the experimentally estimated parameters, to the propagation of a crack located at the T-transition of a generic railway axle, assumed to be built using the two tested steel grades.

Selection and peer-review under responsibility of ICM11

Keywords: ΔK-decreasing, compression pre-cracking, structural steels

1. Introduction

The traditional experimental approaches commonly used for threshold determination, suggested in ASTM E647-05 [1] and named "ΔK-decreasing" and "constant K_{max}", are known to influence the experimental results in a non conservative way [2-5].

In particular, the problems are related to both the adopted pre-cracking methods, which could leave high residual effects in the region near the crack tip, and the procedure of load reduction itself: ASTM E647-05 suggests to begin the load reduction at about 10^{-8} m/cycle, but at this value the SIF value is still high enough to generate load interaction effects, due to plasticity-induced crack closure [6], that can arrest the crack too early. To solve these problems, new approaches [2-5], called CPCA [2] (compression pre-cracking constant amplitude) and CPLR [7] (compression pre-cracking load reduction) have been proposed (Fig.1). These two approaches are both based on a new compression-compression pre-cracking method which produces closure-free and naturally arrested cracks.

* Corresponding author. Tel.: +39 02 2399 8253; fax: +39 02 2399 8263.
E-mail address: daniele.regazzi@mail.polimi.it

Selection and peer-review under responsibility of ICM11 doi:10.1016/j.proeng.2011.04.487

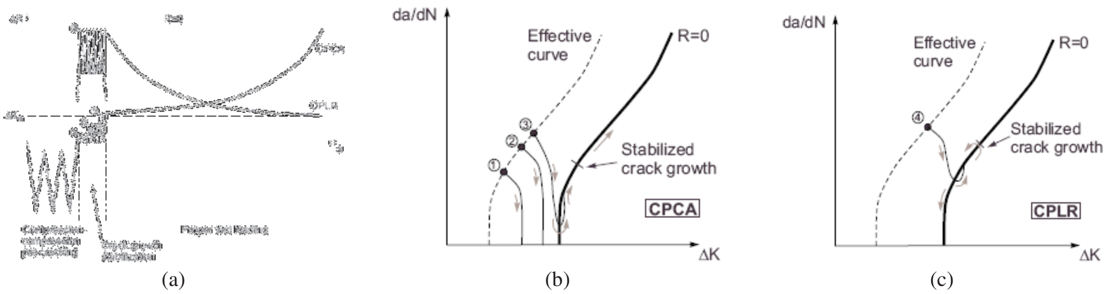

Fig. 1. Compression-compression pre-cracking methods to experimentally generate thresholds: (a) Schematic of the experimental procedures at R=0; (b) CPCA; and (c) CPLR.

In the present research, experiments have been carried out on a low strength normalized C45 and a medium strength 25CrMo4 steel grades, very commonly used as structural steels, in the shape of SE(B) specimens subjected to stress ratios varying from $R=0.75$ (absence of closure phenomena) to $R=-2$.

In order to better explain the consequences a different characterization of the threshold could have on life assessment for a real structure, a simple calculation of life prediction was carried out, considering the case of a railway axle, which is a typical use of these materials. Life assessment is provided in relative terms considering the two Nasgro [8] equations for each material deriving from the two experimental approaches.

2. Compression pre-cracking

Crack propagation tests were carried out on SE(B) specimens (12x24 mm^2 section and 7mm notch).

The standard procedure usually adopted to generate pre-cracking on a notched specimen consists in the application of a SIF higher than the threshold at a given R for a certain amount of cycles needed to obtain an initial crack of about 0.5mm. Because of the pre-cracking procedure itself, the crack develops the plastic wake before starting the test and consequently it already presents some interaction effects. Both these phenomena are known to influence the threshold value deriving from experiments.

Compression pre-cracking was applied to specimens by a four point bending configuration using a servo-hydraulic uniaxial facility with a 100 kN load cell and a dedicated device (Fig.2a and b). The applied load was chosen in order to generate a 130 Nm bending moment at stress ratio $R=10$ and at a frequency of 30 Hz. This bending value was set in order to generate the naturally arrested pre-crack in 10^6 cycles. This number of cycles was defined by regularly checking the pre-crack growth during the first tests by an optical microscope till its natural arrest. The average surface length of the pre-cracks obtained from all the tested specimens was about 0.3 mm (Fig.2c).

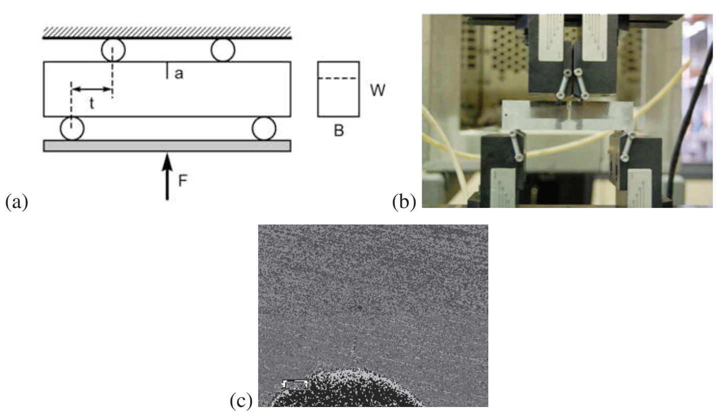

Fig. 2. Compression pre-cracking of SE(B) specimens: (a) schematic of the applied load; (b) experimental set-up; (c) example of a crack resulting from compression pre-cracking.

After compression pre-cracking, specimens were instrumented using two RMF-A10 krak-gages (one for each side and having a measuring base length equal to 10 mm) connected to a Fractomat control unit in order to monitor crack growth in real-time by means of a potential drop technique. The four point bending crack propagation test was carried out by a resonant bending machine having a 160 Nm maximum load and vibrating at approximately 130 Hz.

The tests were carried out on five SE(B) specimens in C45 and fifteen in 25CrMo4 steels, at different stress ratios in order to characterize both the linear part of the crack growth diagram (CPCA test) and the threshold region (CPLR test). In the second case, the typical parameters of the applied loading reduction procedure were set within the limits suggested by ASTM E647-05: the growth rate at which loading reduction was always started was about 10^{-9} m/cycle, and the loading reduction coefficient was set to C=–0.08 mm^{-1}. Truly, the ASTM E647-05 suggests the growth rate at which loading reduction has to be started at about 10^{-8} m/cycle, but this value is known [3] to affect the threshold evaluation since it is high enough to introduce significant load interaction effects (plasticity-induced crack closure [6]). The choice of beginning the load reduction at 10^{-9} m/cycle has been done in order to minimize these effects.

The shape of crack growth curves, adopting compression pre-cracking based methods, became more repeatable with the stress ratio (Fig.3a and 4a): both the fanning (the varying distance between the points of the curves at different *R* in the near-threshold and the linear regions) phenomenon [7] and the different heights of the knees of the sigmoidal, in the transition area between zone I and zone II, typically affecting the results derived from standard procedures, disappeared considering CPCA and CPLR tests. It is also worth noting that the linear regions of the curves were not influenced by the pre-cracking procedure, while the threshold regions were significantly influenced. In particular, a detailed analysis of the trend of thresholds with *R* is shown in Fig.3b (normalized C45 steel) and Fig.4b (25CrMo4 steel) for both compression pre-cracking and traditional procedures. This diagram allows, first of all, to notice that the difference between the results generated by the procedures increased significantly at lower stress ratios, while it was not so important at high *R* values.

3. Nasgro fitting

Data fitting is based on the well-known NASGRO equations (eq.(1)) [8], which represents all the three zones of the Paris diagram; since no experiments were carried out to obtain data about K_c, the third region was neglected from the calculation.

$$\frac{da}{dN} = C\left[\left(\frac{1-f}{1-R}\right)\Delta K\right]^n \frac{\left(1-\frac{\Delta K_{th}}{\Delta K}\right)^p}{\left(1-\frac{K_{max}}{K_c}\right)^q} \tag{1}$$

where *f* is the "Newman closure function" [8] taking into account the stress ratio for long cracks propagation, R is the stress ratio and C, n, p, q are the empirical parameters to determine.

The interpolation of the dependence of ΔK_{th} with *R* has been done on experimental data by the meaning of the NASGRO equation for thresholds [8], shown in eq.(2):

$$\Delta K_{th} = \begin{cases} \Delta K_1 \left(\frac{1-R}{1-f[R]}\right)^{(1-RC_{th}^m)} \Big/ (1-A_0)^{(C_{th}^p - RC_{th}^m)} & if\ R<0 \\ \Delta K_1 \left(\frac{1-R}{1-f[R]}\right)^{(1-RC_{th}^p)} \Big/ (1-A_0)^{(1-R)C_{th}^p} & if\ R\geq 0 \end{cases} \tag{2}$$

where ΔK_1 is the SIF threshold at R=1, while C_{thp} and C_{thm} are the parameters controlling the dependence of ΔK_{th} with R; C_{thp} is valid for positive stress ratios, C_{thm} for the negative ones.

3.1. Normalized C45 steel

In Fig.3a are shown the experiments on C45 steel from both the adopted pre-cracking methods; it's clear that the linear sections are very similar, while the thresholds are quite different. Fig.3b shows the thresholds variation with the stress ratio; the differences are small for *R>0* and become higher for negative values of the stress ratio. That's the case where the interaction effects given from the pre-cracking procedure affect more the results. Fig.3c, in the end, shows the difference between the resulting two curves for the case *R=-1*; the thresholds are different and affect the curve shape, but not significantly.

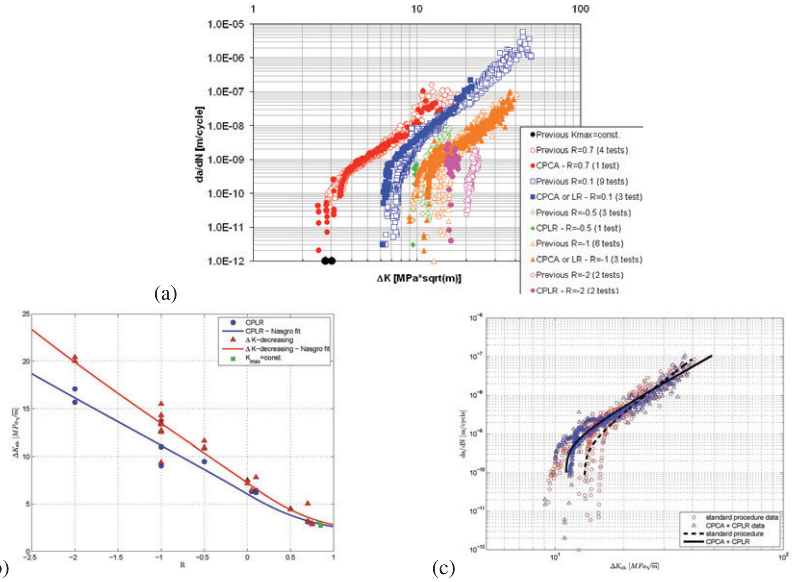

Fig. 3. Comparison between the two methods of pre-cracking for a normalized C45 steel: (a) experimental data; (b) thresholds; (c) Nasgro equations for *R=-1* case.

3.2. 25CrMo4 steel

The behavior is similar for 25CrMo4 steel. The differences of threshold are bigger for negative stress ratios compared to the ones related to C45 steel, as in Fig.4b. Fig.4c shows the comparison between the two pre-cracking methods for *R=-1*. The big difference is in the threshold, while the linear section is more or less the same. In addition, for compression pre-cracking methods the dispersion is smaller.

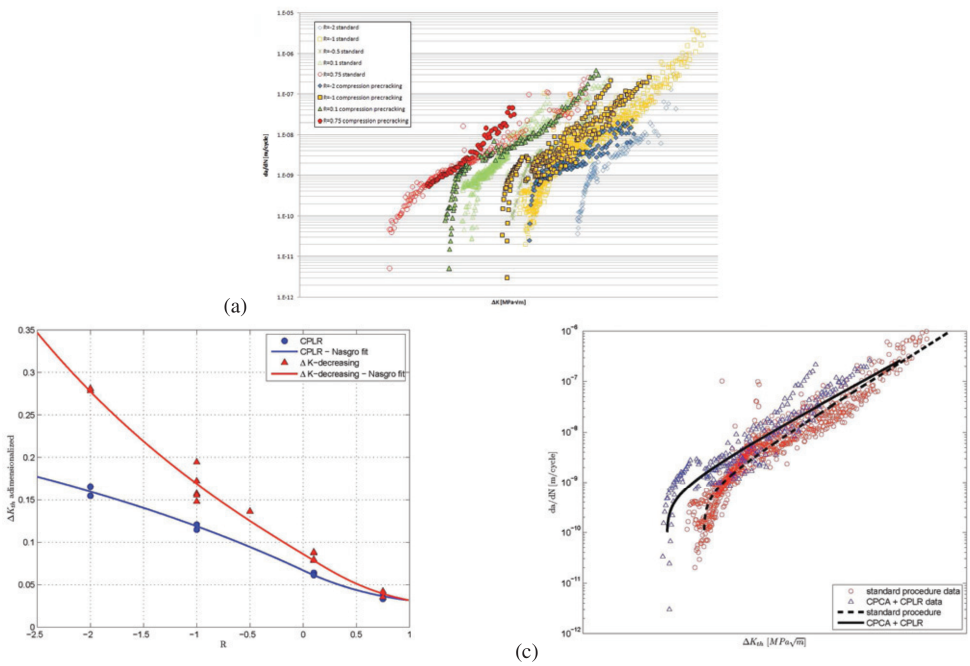

Fig. 4. Comparison between the two methods of pre-cracking for 25CrMo4 steel: (a) experimental data; (b) thresholds; (c) Nasgro equations for *R=-1* case.

4. Comparison between life predictions

The application of compression pre-cracking for determining the thresholds assumes a big importance for all the applications where the typical stress ratio is negative, because of the effects on interval inspections a lower estimated threshold could have. This is, for example, a problem that could interest the estimation of the inspection interval for a railway axle, typically working at R=-1, since the two steels considered are often used for the production of railway axles ([10], [11]). Since the largest part of the life of a common railway axle is spent in the near-threshold region, overestimating the thresholds results in overestimating the cycles the component could afford after the initiation of a crack, for some reason.

An example of calculation of a crack propagation has been carried out considering an initial semi-elliptical crack, with a_0=1mm and a/c=0.6 (a typical crack shape for railway axles). The calculation has been carried out by the meaning of Nasgro equation with the estimated parameters and Shiratori weight functions for a semi-elliptical surface crack in a plate under basic mode of stress distribution [12]. The load spectrum employed is related to the typical service of an underground vehicle. The initial defect for propagation was placed in the T-transition [10] of the axle, where the stresses are typically higher. No residual stresses has been considered; the resulting stress ratio is R=-1 (pure rotating bending).

The diagrams show a big difference in terms of life prediction between the two cases of NASGRO parameters derived by the meaning of traditional experimental procedures (ΔK-decreasing) and CPCA or CPLR experimental procedures. The life prediction carried out is about 5 time shorter for 25CrMo4 material and more than 10 time shorter for normalized C45 steel considering the parameters derived from the compression pre-cracking approach.

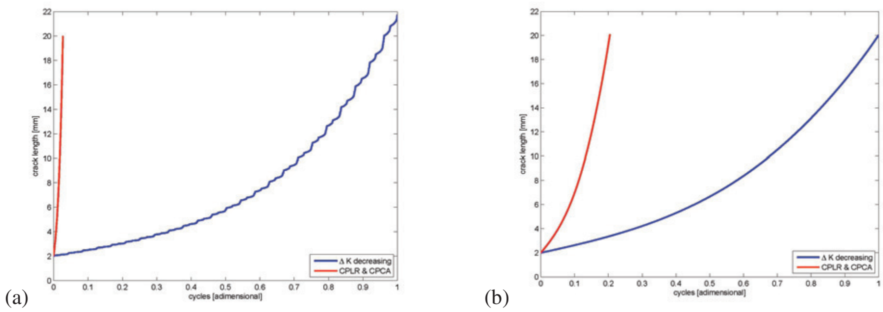

Fig. 5. (a) Crack propagation comparison for C45 normalized steel grade; (b) crack propagation comparison for 25CrMo4 steel grade.

Concluding Remarks

The application of compression pre-cracking testing methods to two common steels for railway axle application, and suitable constant amplitude or load reduction programs, for determining the thresholds SIF and the linear region of the crack propagation rate on SE(B) specimens subjected to stress ratio varying from R=0.75 (absence of closure phenomena) and R=-2, has shown:

- considering the threshold region, traditional approaches based on ΔK-decreasing tests tend to systematically overestimate the threshold SIF, while more conservative results can be obtained from the novel CPCA or CPLR approaches;
- the differences between the evaluated thresholds are almost null for R=0.75, but become larger decreasing the stress ratio to negative ones (about 25% for C45 and more than 60% for 25CrMo4 at R=-2); this can be explained in terms of the closure phenomenon, which assumes more influence as long as R gets lower, making load interaction effects stronger.
- the linear regions do not show these discrepancies and are about indistinguishable from each other;
- a simple application of the Nasgro equation to a crack propagation occurring on a railway axle (T-transition, stress ratio R=-1) by the meaning of the two sets of parameters, shows a big discrepancy in life prediction, yielding non-conservative results with respect to traditional approach results; this has a significant influence on maintenance of railway axles at least in terms of inspection intervals.

Acknowledgements

Part of the present experimental results was obtained in the frame of the MARAXIL (Manufacturing Railway Axles with Improved Lifetime) Project #16973 funded by the Lombardy Regional Council.

References

[1] ASTM E647-05, 2007, "Standard Test Method for Measurement of Fatigue Crack Growth Rates," *Annual Book of ASTM Standards*, Vol. 3_1_, ASTM International, West Conshohocken, PA.

[2] Pippan, R., Stüwe, H. P., and Golos, K., "A Comparison of Different Methods to Determine the Threshold of Fatigue Crack Propagation," *Fatigue*, Vol. 16, 1994, pp. 579–582.

[3] Forth, S. C., Newman, J., Jr., and Forman, R. G., "On Generating Fatigue Crack Growth Thresholds," *Int. J. Fatigue*, Vol. 25, 2003 pp. 9–15.

[4] Forth, S. C., Newman, J., Jr., and Forman, R. G., "Evaluation of Fatigue Crack Thresholds Using Various Experimental Methods," *J. ASTM Int.*, Vol. 2, 2005, Paper ID JAI12847.

[5] Newman, J., Jr., Schneider, J., Daniel, A., and McKnight, D., "Compression Pre-Cracking to Generate Near Threshold Fatigue-Crack-Growth Rates in Two Aluminum Alloys," *Int. J. Fatigue*, Vol. 27, 2005, pp. 1432–1440.

[6] Elber, W., "The Significance of Fatigue Crack Closure," *Damage Tolerance in Aircraft Structure, ASTM STP 486*, ASTM International, West Conshohocken, PA, 1971, pp. 230–242.

[7] Newman, J., Jr. and Yamada, Y., "Compression Pre-Cracking Methods to Generate Near-Threshold Fatigue-Crack-Growth-Rate Data," *17th European Conference on Fracture (ECF17)*, Brno, Czech Republic, 2008.

[8] NASA: *NASGRO 4.0 User Manual*, Website: www.nasgro.swri.org.

[9] UNI EN13104-2009 Railway applications "Wheelsets and bogies - Powered axles Design method".

[10] U. Zerbst, M. Vormwald, C. Andersch, K. Mädler and M. Pfuff, The development of a damage tolerance concept for railway components and its demonstration for a railway axle, *Engng Fract Mech* **72** (2005), pp. 209–239.

[11] M. Shiratori, T. Niyoshi and K. Tanikawa, Analysis of stress intensity factors for surface cracks subjected to arbitrarily distributed surface stress, in: *Stress Intensity Factors Handbook,* Y. Murakami et al., Eds., Vol. 2 (Pergamon: Oxford, 1987).